Laser Speckle Contrast Imaging in Biomedical Optics

Arseny Belousov[1], Dmitry Rudman[1], Yokhai Dan[2], Michal Zivan[1], Rami Shinnawi[2]

[1] Biomedical Engineering Faculty, Technion - IIT, Haifa, Israel
[2] AntiShock, Haifa, Israel

Abstract: Annually, in US, 4.3M critically ill patients in an intensive care unit with various diseases are adversely affected by non-personalized intravenous fluid administration procedures. Managing fluids is done by monitoring hemodynamics. In this paper, we introduce a technology, which can be used for non-invasive continuous micro-hemodynamic monitoring, called laser speckle contrast imaging. We present here a setup we built for simulation of blood flow, imaging system and algorithms used to obtain an indication of tissue perfusion. Using this technology, better flow estimation can be achieved to manage fluids.

Keywords: speckle phenomenon, tissue perfusion, laser speckle contrast imaging

---

1. **Introduction**

Intravenous fluid administration is one of the most common interventions in medicine, widely used to treat various diseases such as sepsis and different shock types. Nowadays, intravenous fluids are not administered in a personalized fashion. In this article we present a different approach for hemodynamic monitoring by an optical imaging technology capable of visualizing capillary blood flow. Existing techniques to image perfusion are: laser Doppler velocimetry and laser speckle contrast analysis[1]. In this work, we utilize interference pattern generated from diffusely backscattered light from the skin, also called - speckle pattern[2]. When there is movement in the object, the speckle pattern statistical properties change. Speckle pattern statistics can be estimated by an optical system consisting a camera, laser and optical filters. By defining long enough camera integration time, static and dynamic areas of the pattern can be seen – which can be referred as level of blurriness. The level of blurring is quantified by regional statistics defined by the speckle contrast. If there is no or little movement in the object, there will be no or only a little blurring.

2. **Background**

2.1 Speckle pattern

Interference pattern on the detector, formed by backscattered light, when an optically rough object is illuminated with coherent laser, called speckle pattern (Figure 1). This pattern consists of dark and bright regions called speckles. When captured on a camera plane, the speckle pattern recorded over

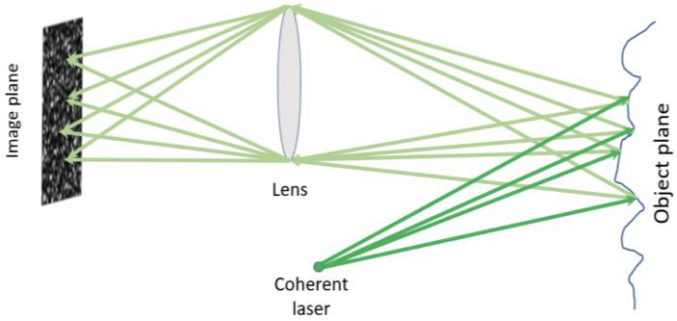

Figure 1. Speckle pattern formation

by finite exposure time of the sensor. The more dynamic the pattern – more blurred it will be presented. The degree of blurring can be measured by regional statistics defined by contrast as follows[3]:

$$K(x,y) = \frac{\sigma_N}{\mu_N}$$

Here μ_N and σ_N are mean and the standard deviation of the pixel intensities in an adjacent area around the pixel. If there is no movement on the surface, the interference pattern does not change over time, we call it – *static speckle pattern*[4]. If the object moves or there is movement within it the interference pattern will change over time, we call it – *dynamic*

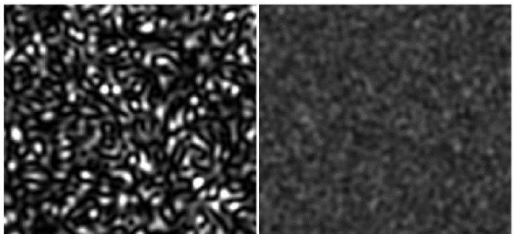

Figure 2. Static (left) and dynamic (right) speckle patterns

speckle pattern, in this case the pattern will be blurred and the standard deviation of intensity will be small, resulting in reduced speckle contrast (Figure 2).

2.2 Speckle dynamic simulation

Quantitative interpretation of the data from such measurement schemes often hinges on accurate knowledge of the spatial and temporal statistical behavior of the speckle phenomenon. To complement experimental measurements, we turned first to computer simulation of the phenomenon. Speckle patterns are simulated by making use of the concept of a *copula concept*: a circular region in a square matrix is filled with complex numbers of unity amplitude and uniformly distributed phases[5]. After Fourier transforming the matrix, and multiplying it point-by-point by its complex conjugate, an artificial speckle pattern is generated. By shifting the circular region with complex numbers one column each time and recalculating the speckle pattern, a dynamic speckle pattern can be generated[6]. The evolution of speckle pattern through frames shown in Figure 3.

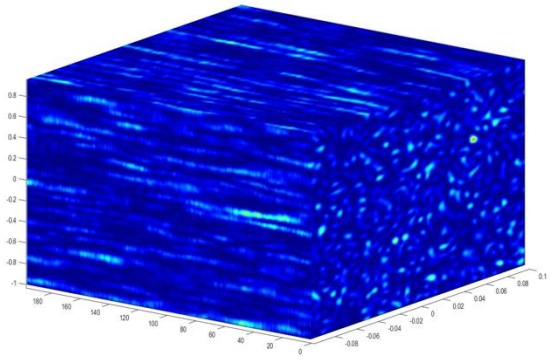

Figure 3. Evolution of speckle pattern.

Simulations of static and dynamic speckle patterns allowed us to determine algorithmically the parameters of interest: speckle size, spatial and temporal contrast, decorrelation and camera exposure times[7].

When we have a sequence of frames with "evolving" speckles we can calculate the correlation function between frames. Decorrelation time can be defined from correlation function[8]. In order to define it we examine a correlation between a frame at specific point in time and frames which comes next to it, we measure a time which takes to correlation function to descent to the pre-defined level, meaning that speckles "evolved" enough and the patterns are not correlated anymore. This parameter is important for determining relation between the contrast value and particle speed. Figure 4 shows correlation function for evolution of speckle patterns which were simulated and shown in Figure 4.

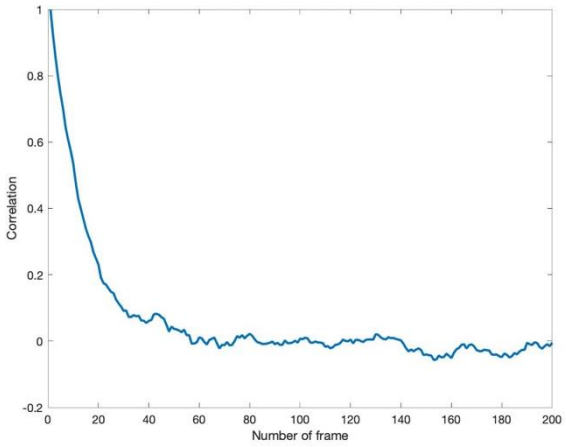

Figure 4. Correlation function of the first frame and frames which comes next

2.3 Speckle size

To obtain good statistics the speckle size should be carefully controlled. When speckle size and pixel size are of the same order, the error in calculated contrast is minimized. In simulations speckle size can be easily controlled by changing parameters in copula. For real image speckle, the speckle size is dependent on the laser wavelength (λ), the f-number of the lens and the magnification (M), as expressed by:

$$d = 2.44 \cdot f_{\#} M$$

Sampling criteria must be satisfied by having the minimum speckle size be two times larger than the camera pixel size, then the Nyquist criteria is met. The optimal size can be chosen by controlling the f-number of the lens system. Validation can be done by finding FWHM and $\frac{1}{e^2}$ (beam waist) values of Gaussian, which fits to two arrays generated by the sums of the normalized autocovariances of all rows in the image and all columns in the image, in this way we can find horizontal and vertical speckle sizes[9].

2.4 Camera exposure time

A finite exposure time is necessary for imaging. Exposure times that are too short would not allow an adequate number of photons to be accumulated, would introduce image noise. A longer exposure

time has the effect of reducing the speckle contrast. Hence, very long exposure times would tend to eliminate the signal, thus deteriorating the final image quality. Between these two extremes, speckle contrast sensitivities as described below become important.

3. **Methods**

3.1 Speckle contrast

In laser speckle contrast imaging setup (Figure 5-a), contrast can be estimated from either the spatial statistics or the temporal statistics. In Laser Speckle Contrast Analysis (LASCA) the contrast is calculated in spatial domain (Figure 5-b), we calculate local contrast for $n \times n$ window by:

$$C_{i,j} = \frac{\sigma}{\mu} = \frac{\sqrt{\frac{1}{(n+1)^2}\sum_{x=i-\frac{n}{2}}^{i-\frac{n}{2}}\sum_{y=j-\frac{n}{2}}^{y+\frac{n}{2}} I_{x,y}^2 - \left(\frac{1}{(n+1)^2}\sum_{x=i-\frac{n}{2}}^{i-\frac{n}{2}}\sum_{y=j-\frac{n}{2}}^{y+\frac{n}{2}} I_{x',y'}\right)^2}}{\frac{1}{(n+1)^2}\sum_{x=i-\frac{n}{2}}^{i-\frac{n}{2}}\sum_{y=j-\frac{n}{2}}^{y+\frac{n}{2}} I_{x,y}}$$

In Laser Speckle Imaging (LSI) the contrast in temporal domain (Figure 5-c) is calculated for 1 pixel in sequence of frames by:

$$C_{i,j} = \frac{\sigma}{\mu} = \frac{\sqrt{\frac{1}{n+1}\sum_{l=t-\frac{n}{2}}^{t-\frac{n}{2}} I_{i,j,l}^2 - \left(\frac{1}{n+1}\sum_{l=t-\frac{n}{2}}^{t-\frac{n}{2}} I_{i,j,l}\right)^2}}{\frac{1}{n+1}\sum_{l=t-\frac{n}{2}}^{t-\frac{n}{2}} I_{i,j,l}}$$

The spatial statistics offers better temporal resolution but at the expense of spatial resolution because of the requirement to use a sufficiently large window of image pixels in the calculation.

The temporal statistics offer better spatial resolution at the expense of temporal resolution[10]. There are techniques which combine calculation of contrast in spatial and temporal domains (Figure 5-d).

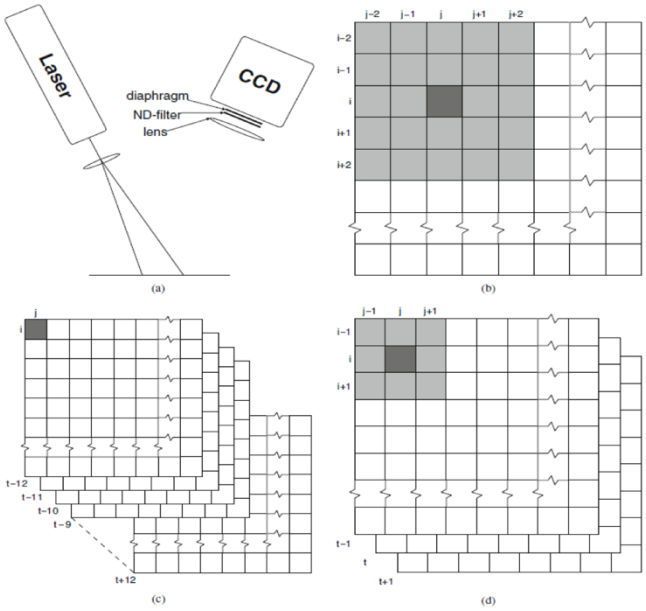

Figure 5. Schematic overview of the ways the contrast is calculated.

In Figure 6 we show implementation of contrast calculating algorithm on simulated speckle patterns. In order to get blurred images, which simulate different exposure times, we summed and normalized a number of neighbouring frames. From a figure we can see that increase in exposure time results in decline of a contrast.

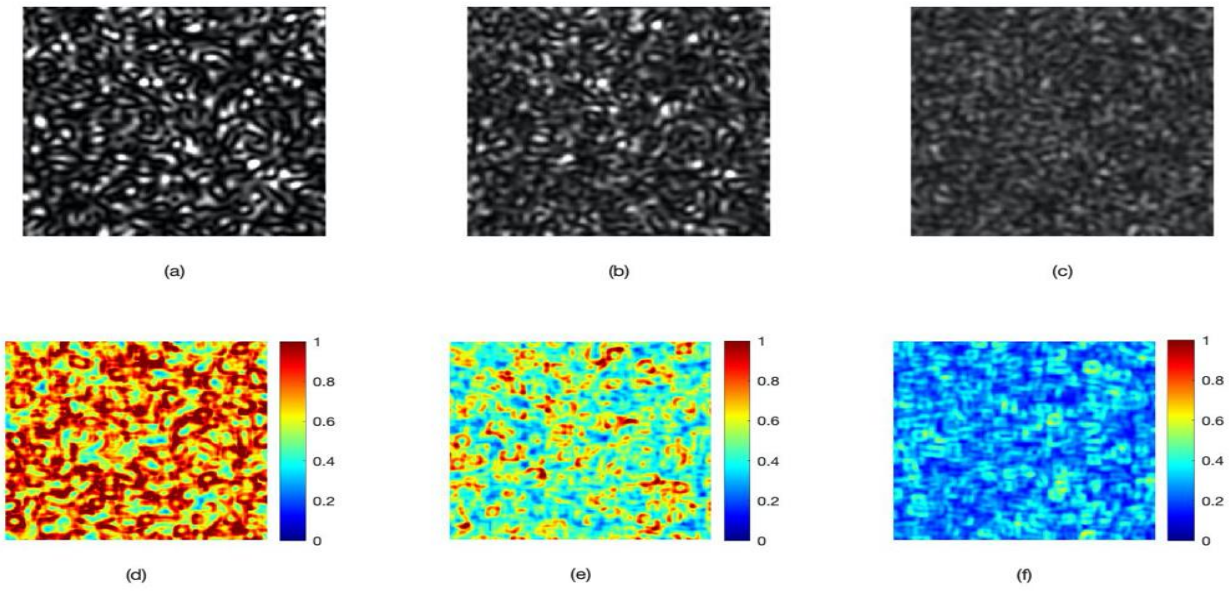

Figure 6. a, b and c Simulated blurred speckle patterns with an exposure time of 1, 5, and 25 ms respectively, d, e, and f conjugated contrast images, with contrast values calculated for 10 x 10 pixels. The contrast value is shown in the colorbar

3.2 Theories relating speckle contrast to particle speed

The precise relationship between the velocity V of scatterers and the decorrelation time τ is not known, but there is evidence that they are inversely proportional and dependent on the wavelength λ of a laser[11]. Commonly, next approximation used:

$$V = \frac{\lambda}{2\pi\tau}$$

The decorrelation time τ can be calculated under the assumption of random Gaussian or Lorentzian velocity distribution from.
The relation between the decorrelation time τ, the exposure time T and the contrast is given by:

$$\frac{\sigma}{\mu} = \sqrt{\frac{\sqrt{\pi}}{2}\frac{\tau}{T}\mathrm{erf}\left(\frac{T}{\tau}\right)} \quad \textit{(Lorentzian velocity distribution)}$$

$$\frac{\sigma}{\mu} = \sqrt{\frac{\sqrt{\pi}}{2T}\left(1 - \mathrm{e}^{\left(-\frac{2T}{\tau}\right)}\right)} \quad \textit{(Gaussian velocity distribution)}$$

4. **Results**

4.1 Experimental setup

In order to measure particle speed experimentally, we build a setup for simulation of capillary blood flow using a syringe pump and a microfluidic chip. As a scattering fluid, we used milk to mimic the blood flow, as the fat particles in milk scatter light similar to red blood cells. Our imaging system comprised of focusing optics, a variable diaphragm and a CMOS sensor. The area of interest was illuminated with a coherent laser ($\lambda \cong 650.$) The digital photography was processed by the computer and the local contrast was computed in spatial and temporal manner.

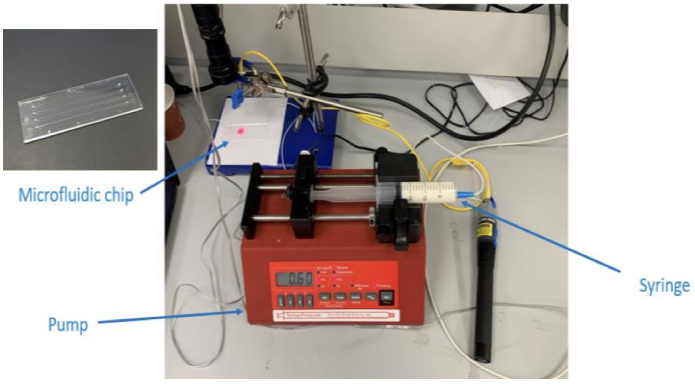

Figure 7. Capillary blood flow simulation setup.

Schematic representation of the setup:

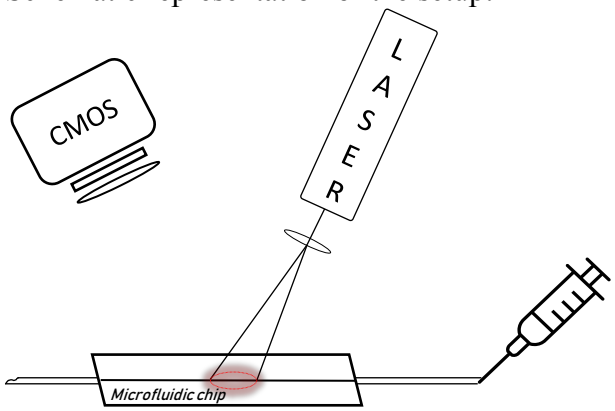

Figure 8. Schematic representation of the setup.

4.2 Implementation of the algorithms

Number of laser speckle contrast techniques were implemented and analysed with our setup and algorithms. In Figure 8 we show the results obtained with LASCA algorithm, for different flow rates we can observe the change in contrast. When there is no flow (zero velocity) we still can observe the change in contrast between static regions and region with fluid under the surface, this change explained by Brownian motion in a fluid.

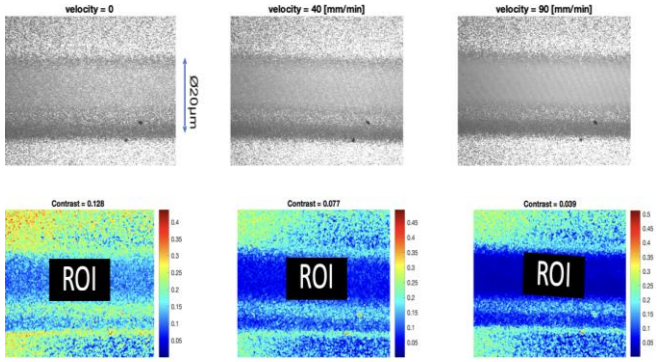

Figure 9. Contrast calculated for different velocities with LASCA algorithm.

In Figure 9 we show a result from another experiment, where we recorded a video of changing flow rates, the goal was to verify the sensitivity of an algorithm at physiological rates. At the same experiment we analyze contrast level from different regions of a pipe. From the difference in a contrast between central and circumferential regions we can conclude that our algorithm is able to distinguish and validate a presence of velocity profile of a fluid in a pipe. Since, the velocity is higher in the centre of the pipe we would expect for lover contrast, because higher velocity results in higher level of dynamics of the surface, which described by lover standard deviation of pixel intensities.

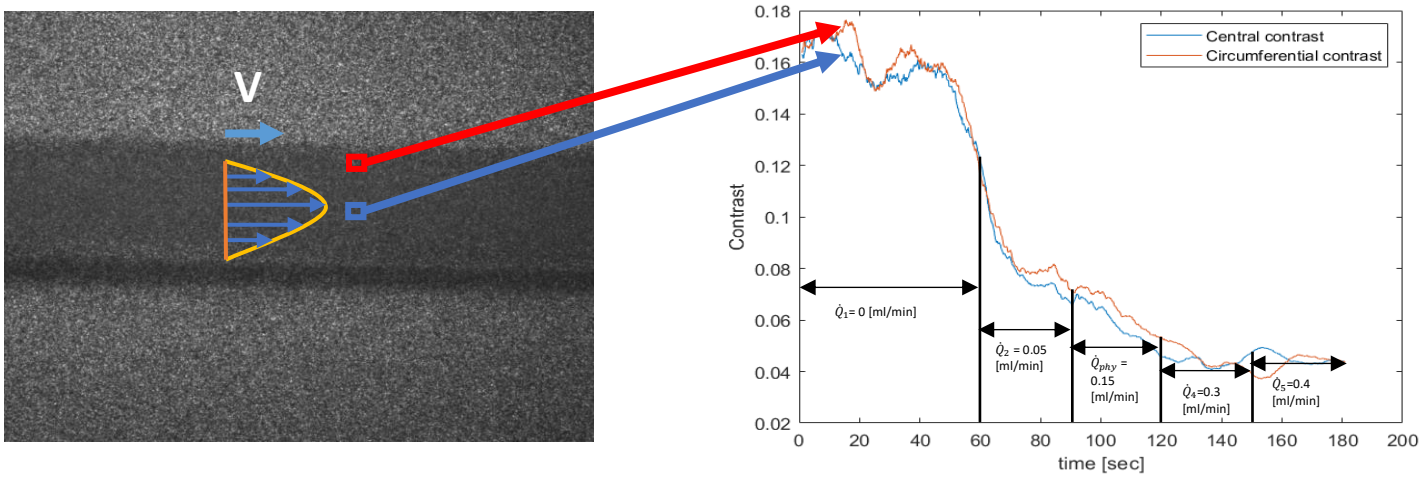

Figure 10. Contrast values at different flow rates at central and circumferential region of a pipe.

At the end we compare between two techniques of contrast calculation in spatial and temporal domain (Figure 10). In spatial domain the contrast is calculated for a window of $15x15$ pixels from a central region of a pipe. In temporal domain the contrast is calculated for a window of $3x3$ pixels and sequence of 9 frames, also from a central region of a pipe. Denoising was made by moving average filter of length 5. In this specific experiment we found that spatial filtering makes a better use for temporal resolution, and results in less noise. This is not a case in physiological surrounding, where spatial information plays a higher role, and temporal or "hybrid" filtering worth consideration.

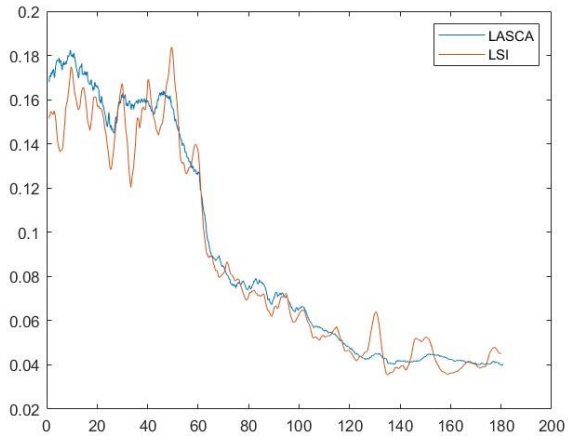

Figure 11. Comparing LASCA to LSI

5. **Conclusions**

Speckle contrast techniques demonstrated its efficiency as a non-invasive real time tool for measuring particle velocity in phantom tube. We have also proved that these techniques are sensitive for small flow rates which allows to observe physical phenomena like velocity profile of a fluid or Brownian motion. Future work can be done to enhance image quality[12], to improve the ability to visualize deep blood vessels using principal component analysis and Kurtosis analysis[13].

6. **Disclosures**

This project in whole was facilitated by AntiShock Technologies LTD, while using its laboratory equipment.

7. **References**

[1] O. B. Thompson and M. K. Andrews, "Tissue perfusion measurements: multiple-exposure laser speckle analysis generates laser Doppler–like spectra," *J. Biomed. Opt.*, vol. 15, no. 2, p. 027015, 2010.

[2] Y. Aizu and T. Asakura, "Bio-speckle phenomena and their application to the evaluation of blood flow," *Opt. Laser Technol.*, 1991.

[3] J. D. Briers, "Laser speckle contrast imaging for measuring blood flow," *Opt. Appl.*, 2007.

[4] J. W. Goodman, "Some fundamental properties of speckle*," *J. Opt. Soc. Am.*, 1976.

[5] D. D. Duncan and S. J. Kirkpatrick, "The copula: a tool for simulating speckle dynamics," *J. Opt. Soc. Am. A*, vol. 25, no. 1, p. 231, 2008.

[6] D. D. Duncan and S. J. Kirkpatrick, "Algorithms for simulation of speckle (laser and otherwise)," *Complex Dyn. Fluctuations Biomed. Photonics V*, vol. 6855, no. May, p. 685505, 2008.

[7] M. Draijer, E. Hondebrink, T. Van Leeuwen, and W. Steenbergen, "Review of laser speckle contrast techniques for visualizing tissue perfusion," *Lasers Med. Sci.*, vol. 24, no. 4, pp. 639–651, 2009.

[8] G. J. Richards and J. D. Briers, “Laser speckle contrast analysis (LASCA): A technique for measuring capillary blood flow using the first order statistics of laser speckle patterns,” *IEE Colloq.*, 1997.

[9] H. Lin and P. Yu, “Speckle mechanism in holographic optical imaging,” *Opt. Express*, 2007.

[10] H. Cheng, Q. Luo, S. Zeng, S. Chen, J. Cen, and H. Gong, “Modified laser speckle imaging method with improved spatial resolution,” *J. Biomed. Opt.*, 2003.

[11] J. Senarathna, A. Rege, N. Li, and N. V. Thakor, “Laser speckle contrast imaging: Theory, instrumentation and applications,” *IEEE Rev. Biomed. Eng.*, vol. 6, pp. 99–110, 2013.

[12] Y. Zhang, Y. Zhao, W. Li, Z. Qian, and L. Xing, “Enhancement of microvessel in laser speckle image using Gaussian kernel template,” *J. Innov. Opt. Health Sci.*, vol. 12, no. 2, pp. 1–10, 2019.

[13] J. A. Arias-Cruz, R. Chiu, H. Peregrina-Barreto, R. Ramos-Garcia, T. Spezzia-Mazzocco, and J. C. Ramirez-San-Juan, “Visualization of in vitro deep blood vessels using principal component analysis based laser speckle imaging,” *Biomed. Opt. Express*, vol. 10, no. 4, p. 2020, 2019.